Dalton
Transactions

Cite this: *Dalton Trans.*, 2012, **41**, 10258

www.rsc.org/dalton

PAPER

Crystal structures and stability of NaLnF$_4$ (Ln = La, Ce, Pr, Nd, Sm and Gd) studied with synchrotron single-crystal and powder diffraction†

Andrzej Grzechnik*[a] and Karen Friese[b]

Received 21st March 2012, Accepted 4th June 2012
DOI: 10.1039/c2dt30650f

Crystal structures of the NaLnF$_4$ materials (Ln = La, Ce, Pr, Nd, Sm or Gd) were studied with synchrotron single-crystal and powder diffraction. The materials with Ln = La, Ce, Nd, Sm and Gd have the average β structure ($P\bar{6}$, $Z = 1$) with partial ordering of the cations. A new type of a superstructure due to ordering of the cations and vacancies was found in NaPrF$_4$ ($P3$, $Z = 6$). It could be described using the group–subgroup relationships $P\bar{6} \leftrightarrow P3$. Our observations suggest that the β structure is unstable and that the ordering is a slow process at ambient conditions. Upon compression, β-NaNdF$_4$, β-NaGdF$_4$ and the superstructure NaPrF$_4$ are stable to at least 8 GPa with no evidence for any pressure-induced disorder–order phenomena.

Introduction

The most efficient host material for green and blue upconversion known to date is hexagonal NaYF$_4$ doped with lanthanides.[1] It is widely used, for instance, in optical fibers, solar cells and immunoassay detectors. Different synthesis methods and upconversion processes in the bulk, nanocrystalline and colloidal materials have been extensively studied over last decades. Efficient upconversion is also observed in various other MXF$_4$ host lattices (M = Li, Na or K; X = rare earth or Y).

The high efficiency of the upconversion in the NaXF$_4$ compounds is related to the multisite character of their crystal structure.[1–3] The structure of the NaXF$_4$ compounds at room temperature, *i.e.*, of the β polymorphs, is described in space group $P\bar{6}$.[4] Three cationic sites (Wyckoff positions, WP) can be distinguished. Two of them, [WP1*f*] and [WP1*a*], are coordinated by nine F$^-$ ions forming capped trigonal prisms around X^{3+}. The site [WP1*f*] shows occupational disorder and is populated by Na$^+$ and X^{3+} in the ratio of 1 : 1. The site [WP1*a*] is fully occupied by X^{3+}. The third cationic site [WP2*h*] with an irregular octahedral coordination is only half occupied by Na$^+$.

The cationic disorder is expressed by diffuse layers perpendicular to c^*, which show a honeycomb-like intensity distribution in the (a^*,b^*) plane.[2] The diffuse scattering was interpreted as due to the presence of columns of cations in the structure, which are characterized by translational order along the c direction, while these columns show a disordered arrangement in the (a,b) plane. In addition, one of the fluorine atom positions is displaced away from the Na$^+$ ion towards the X^{3+} ion with respect to the Wyckoff position 1*f*.

It was shown that the β phases with Y and heavier lanthanides transform to the fluorite-type α structure (space group $Fm\bar{3}m$) at about 900–1000 K.[5] The transition temperature depends on the size of the X^{3+} cation. In contrast to the hexagonal phases, where partial ordering of the cations exists, the cubic α phases are characterized by complete cationic disorder.

Previously, we investigated LiYF$_4$,[6] LiGdF$_4$,[7] and LiLuF$_4$[8] scheelite host lattices at high pressures. Their crystal structure (space group $I4_1/a$) with a complete ordering of the cations is derived from that of fluorite. Their actual behaviour is closely related to the radii of the X^{3+} cations. In LiYF$_4$, apart from the scheelite → fergusonite transformation at about 11 GPa, another structural transformation above 17 GPa to an undetermined phase was detected.[6] LiGdF$_4$ scheelite decomposes above 11 GPa.[7] At 10.7 GPa, LiLuF$_4$ reversibly transforms to the fergusonite structure.[8] No other phase transition is observed up to 19.5 GPa.

To our knowledge, the only published studies on the high-pressure structural behaviour of the NaXF$_4$ compounds so far are those on NaYF$_4$, in which high-pressure synchrotron powder diffraction experiments were performed both on the cubic and the hexagonal polymorphs.[9,10] In the β polymorph, a pressure-induced phase transition at about 20 GPa involving subtle changes in the diffraction pattern was observed.[9] However, no reliable result concerning the space group symmetry and structure of the high-pressure phase could be obtained, and both the gagarinite (space group $P6_3/m$)[11] and β-Na$_2$ThF$_6$ (space group $P321$)[12,13] structures were suggested as possible candidates for the high-pressure polymorph. Luminescence measurements on β-NaYF$_4$:Er^{3+},Yb^{3+} demonstrated that the upconversion is still highly efficient on compression to 30 GPa due to the stability of the multisite structure.[3] The high-pressure studies on α-NaYF$_4$ documented a phase transition above 10 GPa to a new polymorph, which seems to be of the gagarinite type ($P6_3/m$) with partial ordering of the cations.[10] The occurrence of the phase

---

[a] *Institute of Crystallography, RWTH Aachen, 52066 Aachen, Germany. E-mail: grzechnik@xtal.rwth-aachen.de*
[b] *Jülich Centre for Neutron Science, 52425 Jülich, Germany*

† Electronic supplementary information (ESI) available. See DOI: 10.1039/c2dt30650f

transitions in both polymorphs implies a change of the degree of cationic (dis)order under pressure.[9,10]

In this study we are interested in further structural investigations of the β-$NaLnF_4$ compounds (Ln = La, Ce, Pr, Nd, Sm or Gd) at ambient and high pressures using synchrotron radiation. The high brilliance of synchrotron radiation has the advantage of improved peak-to-background ratio. It facilitates the detection of weak reflections that are difficult to be observed on a home diffractometer. In addition, the use of synchrotron radiation allows measurements at higher energies when compared to the laboratory sources and thus facilitates access to a larger fraction of the reciprocal space in the high-pressure single-crystal experiments using diamond anvil cells.

Experimental

The crystals were grown by the Czochralski method by Jean-Yves Gesland (Le Mans, France). The ones with La, Ce, Pr, Sm and Gd were previously studied with vibrational spectroscopy by Lage *et al.*[14]

The synchrotron experiments at ambient (λ = 0.3978 Å) and high pressures (λ = 0.4000 Å) were performed on the beamline D3 at HASYLAB (Hamburg, Germany) equipped with a HUBER four-circle diffractometer and a marCCD165 detector. The sizes of the crystals were approximately 30 × 50 × 60 μm. The high-pressure single-crystal data were collected in the Ahsbahs[15] and Boehler–Almax[16] diamond anvil cells at room temperature. For all the single-crystal measurements, the intensities were indexed and integrated using the program XDS.[17] A numerical absorption correction was applied to all datasets with the program Jana2006.[20] Further data treatment was carried out according to the procedures described by Friese *et al.*[18] and Posse *et al.*[19] Structure refinements were carried out with the program Jana2006.[20]‡

Powder X-ray measurements at high pressures and room temperature were also carried out using the same diffractometer and detector on the beamline D3. A finely ground sample of β-$NaNdF_4$ was loaded into the Boehler–Almax[16] diamond anvil cell for powder experiments with monochromatic radiation at 0.4 Å. The images were integrated with the program FIT2D to yield intensity *versus* 2θ diagrams.[21] A fluorite powder was added as an internal standard for the 2θ calibration at each pressure through the CaF_2 equation of state.[22]

During all the high-pressure experiments, a 4 : 1 mixture of methanol and ethanol was used as the pressure medium and the ruby luminescence method[23] was used for pressure calibration.

Results and discussion

Ambient pressure

The datasets for Ln = La, Ce, Nd, Sm and Gd measured at ambient pressure can be indexed with unit cells of approximately $a \sim 6.1$ Å and $c \sim 3.8$ Å.[2] On the other hand, in the dataset for $NaPrF_4$, weak superstructure reflections are observed. These additional reflections can be indexed with a large unit cell with a = 10.617(1) Å and c = 7.499(5) Å. The transformation from the average structure to the larger superstructure cell is given by the relationships $a_{\text{super}} = 2a + b$, $b_{\text{super}} = -a + b$, and $c_{\text{super}} = 2c$. For the atomic coordinates an additional origin shift of (2/3,1/3,0) has to be taken into account.

For the datasets which can be described using the small unit cell (Ln = La, Ce, Nd, Sm and Gd), averaging of the data with different point group symmetry suggested the space groups corresponding to Laue symmetry $6/m$ or $\bar{3}$. No systematic extinctions were observed implying space groups $P3$, $P\bar{3}$, $P6$, $P\bar{6}$ or $P6/m$. Trial refinements were carried out in all these space groups using the atomic coordinates from ref. 2 as a basis for the starting models. According to the Hamilton tests[24,25] the space group $P\bar{6}$ was superior in each case in agreement with the earlier investigations.[2]

As twinning is very common in fluoride compounds[12,26,27] and space group $P\bar{6}$ allows for merohedral twinning of the type II, the corresponding twin models were checked in all the datasets. However, in none of the twin refinements was a second twin individual with a significant volume fraction observed.

In the refinements, all atoms were treated anisotropically in the average β structures at ambient pressure. Coordinates and displacement parameters of Na and the respective rare earth ion occupying the same position were restrained to be equal. Initially, the occupational parameters of the two ions were refined. However, the occupations did not show a significant deviation from the ratio of 1 : 1 so that the ideal values were fixed in all the final refinements. Tables 1–3 present all the experimental details and the results of our final refinements of the average structures at ambient conditions. The distances Ln–F and (Na,Ln)–F along the series of atoms Ln = La, Ce, Pr, Nd, Sm and Gd are shown in Table 3.

The data set for $NaPrF_4$ was first refined assuming the average β structure (Tables 1–3). For the superstructure, internal agreement factors are better for Laue symmetry $\bar{3}$ than for $6/m$. Trial refinements of the models obtained from the group–subgroup relationships with respect to the average structure in $P\bar{6}$ were performed in different corresponding space groups ($P3$, $P\bar{3}$, $P6$, $P\bar{6}$ and $P6/m$) and the results were compared with Hamilton tests.[24,25] In this case, space group $P3$ led to the best result. The symmetry reduction $P\bar{6} \rightarrow P3$ from the average β structure to the superstructure involves the loss of a 2-fold rotation around the c axis. The introduction of this symmetry operation as an additional twinning element considerably improved the overall agreement factor, which lowered more than 5%. The refined volume fractions for both individuals in the final refinement are 0.499(2) and 0.501(2).

To avoid correlations, the displacement parameters of the atoms, which are equivalent in the average structure and related by pseudo-centering operations, were restricted to be equal. The pseudo-centering operations were defined as local symmetry operations. The initial refinement demonstrated that the atomic positions with mixed occupancies of Na^+ and Pr^{3+}, with the only exception of the Na2f/Pr2f position, showed no significant deviations from the ideal positions. Consequently these atoms were fixed to the ideal positions. The introduction of these positional restraints did not have a significant effect on the overall

---

‡ Further details of all the crystallographic investigations at ambient and high pressures can be obtained from the Fachinformationszentrum Karlsruhe, D-76344 Eggenstein-Leopoldshafen, Germany, on quoting the depository numbers CSD 424379–424393.

Table 1 Experimental details for β-$NaXF_4$ with the average structure at ambient pressure – space group $P\bar{6}$, $Z = 1$

Material	β-$NaLaF_4$	β-$NaCeF_4$	β-$NaPrF_4$	β-$NaNdF_4$	β-$NaSmF_4$	β-$NaGdF_4$
Crystal data						
a (Å)	6.180(1)	6.153(2)	6.130(1)	6.1090(7)	6.071(2)	6.040(1)
c (Å)	3.8310(5)	3.785(1)	3.7495(5)	3.7160(5)	3.660(2)	3.6100(6)
V (Å^3)	126.71(3)	124.10(7)	122.01(3)	120.10(3)	116.82(8)	114.05(3)
ρ (g cm^{-3})	4.68	4.80	4.90	5.05	5.31	5.59
λ (Å)	0.3978	0.3978	0.3978	0.3978	0.3978	0.3978
μ (mm^{-1})	2.637	2.963	3.124	3.388	4.006	4.664
G_{iso}	0.22(2)	0.17(4)	0.30(4)	0.32(5)	0.37(12)	0.33(8)
Data collection						
No. measured refl.	2836	2777	2647	2581	2991	2981
No. observed refl.[a]	1011	968	978	915	724	870
h_{min},h_{max}	−11,13	−12,10	−13,9	−9,13	−11,12	−12,13
k_{min},k_{max}	−13,12	−12,12	−12,13	−13,13	−7,13	−13,12
l_{min},l_{max}	−8,8	−8,8	−8,5	−7,6	−7,8	−6,7
$R(\mathrm{int})_{obs/all}$[b]	3.44/3.44	3.51/3.52	6.75/6.75	3.03/3.03	4.80/4.80	3.97/3.99
Refinement						
$R_{obs/all}$	2.53/2.55	2.52/2.97	2.97/3.83	2.30/3.27	4.74/6.23	3.42/5.86
w$R_{obs/all}$	3.36/3.36	2.60/2.98	2.97/3.83	2.31/3.28	4.74/6.23	3.64/5.92
GoF$_{obs/all}$	2.16/2.15	1.25/1.24	1.54/1.54	0.79/0.79	4.42/4.42	1.58/1.55
No. parameters	21	21	21	21	21	21

[a] The criterion for observed reflections is $|F_{obs}| > 3\sigma$. [b] All agreement factors are given in %; weighting scheme $1/[\sigma^2(F_{obs}) + (0.01F_{obs})^2]$.

Table 2 Atomic coordinates and isotropic displacement parameters in β-$NaXF_4$ with the average structure at ambient pressure – space group $P\bar{6}$, $Z = 1$

Compound	Atom	x	y	z	Occ.	U_{iso}
$NaLaF_4$	La1	0	0	0	1	0.00981(4)
$NaCeF_4$	Ce1	0	0	0	1	0.00921(3)
$NaPrF_4$	Pr1	0	0	0	1	0.00787(4)
$NaNdF_4$	Nd1	0	0	0	1	0.00916(4)
$NaSmF_4$	Sm1	0	0	0	1	0.00869(8)
$NaGdF_4$	Gd1	0	0	0	1	0.0100(1)
$NaLaF_4$	Na1	1/3	2/3	0.646(3)	0.5	0.044(2)
$NaCeF_4$	Na1	1/3	2/3	0.662(2)	0.5	0.032(1)
$NaPrF_4$	Na1	1/3	2/3	0.670(3)	0.5	0.032(2)
$NaNdF_4$	Na1	1/3	2/3	0.648(3)	0.5	0.037(2)
$NaSmF_4$	Na1	1/3	2/3	0.637(8)	0.5	0.047(7)
$NaGdF_4$	Na1	1/3	2/3	0.581(3)	0.5	0.020(2)
$NaLaF_4$	Na2/La2	2/3	1/3	1/2	0.5/0.5	0.00949(7)
$NaCeF_4$	Na2/Ce2	2/3	1/3	1/2	0.5/0.5	0.01140(7)
$NaPrF_4$	Na2/Pr2	2/3	1/3	1/2	0.5/0.5	0.01060(9)
$NaNdF_4$	Na2/Nd2	2/3	1/3	1/2	0.5/0.5	0.00966(7)
$NaSmF_4$	Na2/Sm2	2/3	1/3	1/2	0.5/0.5	0.0088(2)
$NaGdF_4$	Na2/Gd2	2/3	1/3	1/2	0.5/0.5	0.0047(1)
$NaLaF_4$	F1	0.6304(6)	0.0406(7)	0	1	0.028(1)
$NaCeF_4$	F1	0.6314(7)	0.0409(7)	0	1	0.027(1)
$NaPrF_4$	F1	0.6334(6)	0.0409(7)	0	1	0.024(1)
$NaNdF_4$	F1	0.6350(6)	0.0430(6)	0	1	0.026(1)
$NaSmF_4$	F1	0.6374(18)	0.04558(19)	0	1	0.024(2)
$NaGdF_4$	F1	0.6393(12)	0.0488(13)	0	1	0.030(2)
$NaLaF_4$	F2	0.7308(4)	0.7536(4)	1/2	1	0.0152(6)
$NaCeF_4$	F2	0.7320(4)	0.7547(4)	1/2	1	0.0150(6)
$NaPrF_4$	F2	0.7328(5)	0.7552(4)	1/2	1	0.0138(6)
$NaNdF_4$	F2	0.7335(4)	0.7553(4)	1/2	1	0.0146(5)
$NaSmF_4$	F2	0.7354(11)	0.7570(11)	1/2	1	0.0139(14)
$NaGdF_4$	F2	0.7333(8)	0.7536(8)	1/2	1	0.0125(11)

agreement factor, but it considerably reduced the errors of the refined parameters. However, in the case of the atomic positions Na2f/Pr2f, the difference Fourier synthesis clearly revealed additional maxima, so that for these two atoms the positional parameters were refined independently. All displacement parameters for the Na^+ and Pr^{3+}, which occupy the same Wyckoff position, were restrained to be equal.

The occupational parameters of each pair of atoms Na/Pr were allowed to vary freely with the only restriction that their sum would be equal to the ideal occupancy. The overall composition

Table 3 Selected distances (Å) in β-NaXF_4 (X = La, Ce, Pr, Nd, Sm, and Gd) with the average structure at ambient pressure – space group $P\bar{6}$, $Z = 1$

Compound	$NaLaF_4$	La1	–F1	(3×)	2.419(5)
	$NaCeF_4$	Ce1	–F1	(3×)	2.404(5)
	$NaPrF_4$	Pr1	–F1	(3×)	2.383(5)
	$NaNdF_4$	Nd1	–F1	(3×)	2.372(4)
	$NaSmF_4$	Sm1	–F1	(3×)	2.353(13)
	$NaGdF_4$	Gd1	–F1	(3×)	2.340(9)
	$NaLaF_4$	La1	–F2	(6×)	2.494(1)
	$NaCeF_4$	Ce1	–F2	(6×)	2.468(2)
	$NaPrF_4$	Pr1	–F2	(6×)	2.448(2)
	$NaNdF_4$	Nd1	–F2	(6×)	2.430(1)
	$NaSmF_4$	Sm1	–F2	(6×)	2.395(5)
	$NaGdF_4$	Gd1	–F2	(6×)	2.381(4)
	$NaLaF_4$	Na1	–F1	(3×)	2.511(7)
	$NaCeF_4$	Na1	–F1	(3×)	2.465(6)
	$NaPrF_4$	Na1	–F1	(3×)	2.440(7)
	$NaNdF_4$	Na1	–F1	(3×)	2.480(7)
	$NaSmF_4$	Na1	–F1	(3×)	2.495(19)
	$NaGdF_4$	Na1	–F1	(3×)	2.601(9)
	$NaLaF_4$	Na1	–F2	(3×)	2.306(4)
	$NaCeF_4$	Na1	–F2	(3×)	2.315(4)
	$NaPrF_4$	Na1	–F2	(3×)	2.317(4)
	$NaNdF_4$	Na1	–F2	(3×)	2.291(5)
	$NaSmF_4$	Na1	–F2	(3×)	2.274(10)
	$NaGdF_4$	Na1	–F2	(3×)	2.220(5)
	$NaLaF_4$	(Na2,La2)	–F1	(6×)	2.566(3)
	$NaCeF_4$	(Na2,Ce2)	–F1	(6×)	2.545(3)
	$NaPrF_4$	(Na2,Pr2)	–F1	(6×)	2.531(3)
	$NaNdF_4$	(Na2,Nd2)	–F1	(6×)	2.509(3)
	$NaSmF_4$	(Na2,Sm2)	–F1	(6×)	2.473(8)
	$NaGdF_4$	(Na2,Gd2)	–F1	(6×)	2.440(6)
	$NaLaF_4$	(Na2,La2)	–F2	(3×)	2.424(3)
	$NaCeF_4$	(Na2,Ce2)	–F2	(3×)	2.417(3)
	$NaPrF_4$	(Na2,Pr2)	–F2	(3×)	2.409(3)
	$NaNdF_4$	(Na2,Nd2)	–F2	(3×)	2.400(3)
	$NaSmF_4$	(Na2,Sm2)	–F2	(3×)	2.391(8)
	$NaGdF_4$	(Na2,Gd2)	–F2	(3×)	2.363(5)

Table 4 Experimental details for the $NaPrF_4$ superstructure at ambient pressure – space group $P3$, $Z = 6$

Crystal data	
a (Å)	10.617(1)
c (Å)	7.499(5)
V (Å^3)	732.04
ρ (g cm^{-3})	4.90
λ (Å)	0.3978
μ (mm^{-1})	3.133
G_{iso}	0.10(1)
Data collection	
No. measured refl.	15 844
No. of symmetry independent reflections	9130
No. observed refl.^{a}	3085
h_{min}, h_{max}	−23,22
k_{min}, k_{max}	−22,14
l_{min}, l_{max}	−12,16
$R(\text{int})_{obs/all}{}^b$	5.40/6.14
Refinement	
$R_{obs/all}$	4.16/14.27
$wR_{obs/all}$	5.56/6.58
$\text{GoF}_{obs/all}$	1.47/1.01
No. parameters	83

[a] The criterion for observed reflections is $|F_{obs}| > 3\sigma$. [b] All agreement factors are given in %; weighting scheme $1/[\sigma^2(F_{obs}) + (0.01F_{obs})^2]$.

Table 5 Atomic coordinates and isotropic displacement parameters in the $NaPrF_4$ superstructure at ambient pressure – space group $P3$, $Z = 6$

Atom	x	y	z	Occupancy	U_{iso}
Pr1a	−0.33127(6)	0.00030(11)	0		0.00842(19)
Pr1b	−0.33523(7)	−0.00023(11)	0.5		0.00842(19)
Na1a	−0.3388(7)	−0.3379(7)	0.1682(11)		0.032(2)
Na1b	−0.3258(6)	−0.3305(6)	0.6683(11)		0.032(2)
Pr2a	−0.3333	−0.6667	0.25912(4)	0.115(4)	0.00788(8)
Na2a	−0.3333	−0.6667	0.25912(4))	0.219(4)	0.00788(8)
Pr2b	−0.3333	−0.6667	0.75912(4)	0.210(4)	0.00788(8)
Na2b	−0.3333	−0.6667	0.7591	0.124(4)	0.00788(8)
Pr2c	−0.6667	−0.3333	0.25912(4)	0.109(4)	0.00788(8)
Na2c	−0.6667	−0.3333	0.25912(4)	0.224(4)	0.00788(8)
Pr2d	−0.6667	−0.3333	0.7591	0.214(4)	0.00788(8)
Na2d	−0.6667	−0.3333	0.7591	0.119(4)	0.00788(8)
Pr2e	0	0	0.25912(4)	0.266(2)	0.00788(8)
Na2e	0	0	0.2591	0.067(2)	0.00788(8)
Pr2f	0	0	0.7591	0.094(1)	0.00788(8)
Na2f	0.0350(15)	−0.0270(15)	0.7591	0.239(1)	
F1a	−0.2542(7)	−0.4752(7)	0.0078(9)		0.0115(5)
F1b	−0.2601(6)	−0.4857(6)	0.5295(10)		0.0115(5)
F1c	−0.5841(7)	−0.1412(7)	0.0073(9)		0.0115(5)
F1d	−0.5967(6)	−0.1539(6)	0.5273(10)		0.0115(5)
F1e	−0.9231(6)	−0.8112(6)	0.0294(9)		0.0115(5)
F1f	−0.9277(7)	−0.8223(6)	0.5177(7)		0.0115(5)
F2a	−0.4973(8)	−0.5713(8)	0.2562(14)		0.0138(5)
F2b	−0.4933(8)	−0.5673(8)	0.7588(15)		0.0138(5)
F2c	−0.8316(8)	−0.2394(8)	0.2580(14)		0.0138(5)
F2d	−0.8269(8)	−0.2348(8)	0.7571(14)		0.0138(5)
F2e	−0.1618(8)	−0.8999(8)	0.2637(14)		0.0138(5)
F2f	−0.1663(7)	−0.9109(7)	0.7550(13)		0.0138(5)

as resulting from the refinement, $Na_{1.496}Pr_{1.504}F_6$, is within errors identical to the ideal value of $Na_{1.5}Pr_{1.5}F_6$.

A detailed analysis of the superstructure in $NaPrF_4$ with space group symmetry $P3$ (Tables 4–7 and Fig. 1) reveals the following:§

(1) For the atomic positions which are fully occupied by Pr^{3+}, the displacements from the ideal positions resulting from the transformed average structure are very small (the maximum displacement is less than 0.04 Å).

(2) For nearly all the atomic positions which are occupied by both Pr^{3+} and Na^+, there are no significant deviations from the ideal positions which result from the transformation of the average structure using the group–subgroup relationship. However, for the pair Na2f/Pr2f, two slightly different atomic positions have to be introduced: the Pr^{3+} position coincides with the 3-fold axis, while the Na^+ position is slightly displaced from the 3-fold axis.

(3) In the β average structure, the position [WP1*f*] which incorporates both Na^+ and Pr^{3+} shows occupation probabilities of 0.5 : 0.5. In the superstructure, this position splits into six positions, all of them with mixed occupancies. Three of them are predominantly occupied by Pr^{3+}, the other three are predominantly populated by Na^+. For all of them, the sum of the occupation probabilities, occ(Na) + occ(Pr), was restrained to be 0.3333, *i.e.*, to the full overall occupation. However, no restrictions were introduced which relate the individual positions. Still,

---

§ An analysis of the relationship between the average structure and the superstructure using distortion modes is available in the ESI.† It has been performed using the program ISODISTORT.[28]

Table 6 Selected distances (Å) in the $NaPrF_4$ superstructure at ambient pressure – space group $P3$, $Z = 6$

Pr1a	–F1a		2.392(9)	Pr1b	–F1b		2.391(8)
	–F1c		2.357(8)		–F1d		2.393(7)
	–F1e		2.378(14)		–F1f		2.388(15)
	–F2a		2.480(8)		–F2a		2.349(8)
	–F2b		2.471(9)		–F2b		2.519(9)
	–F2c		2.479(7)		–F2c		2.335(7)
	–F2d		2.464(7)		–F2d		2.518(7)
	–F2e		2.527(6)		–F2e		2.340(6)
	–F2f		2.439(6)		–F2f		2.468(6)
Na1a	–F1a		2.402(14)	Na1b	–F1b		2.330(14)
	–F1c		2.363(14)		–F1d		2.386(14)
	–F1e		2.369(12)		–F1f		2.389(12)
	–F2a		2.326(8)		–F2b		2.316(8)
	–F2c		2.380(12)		–F2d		2.303(12)
	–F2e		2.383(10)		–F2f		2.283(9)
Pr2a/ Na2a	–F1a	(3×)	2.506(9)	Pr2b/ Na2b	–F1a	(3×)	2.556(9)
	–F1b	(3×)	2.629(9)		–F1b	(3×)	2.446(9)
	–F2a	(3×)	2.439(7)		–F2b	(3×)	2.364(7)
Pr2c/ Na2c	–F1c	(3×)	2.521(9)	Pr2d/ Na2d	–F1c	(3×)	2.576(9)
	–F1d	(3×)	2.637(9)		–F1d	(3×)	2.446(9)
	–F2c	(3×)	2.443(7)		–F2d	(3×)	2.370(7)
Pr2e/ Na2e	–F1e	(3×)	2.427(9)	Pr2f	–F1e	(3×)	2.656(9)
	–F1f	(3×)	2.527(9)		–F1f	(3×)	2.552(9)
	–F2e	(3×)	2.466(7)		–F2f	(3×)	2.357(7)
Pr2f	–Na2f		0.598(19)	Na2f	–F1e		2.988(17)
Na2f	–Na2f		1.01(3)		–F1e		2.991(16)
					–F1e		2.437(17)
					–F1f		2.712(18)
					–F1f		2.721(16)
					–F1f		2.093(18)
					–F2f		2.94(2)
					–F2f		2.102(15)
					–F2f		2.150(13)

Table 7 Refined occupational parameters (Occ.) and bond valence sums (BVS) for the Pr^{3+} and Na^+ cations in the $NaPrF_4$ superstructure at ambient pressure – space group $P3$, $Z = 6$

Position	Occ.: Pr	Occ.: Na	BVS: Pr	BVS: Na
2a	0.115(4)	0.219	2.28(2)	0.898(8)
2b	0.210(4)	0.124	2.82(2)	1.110(9)
2c	0.109(4)	0.224	2.31(2)	0.909(8)
2d	0.214(4)	0.119	2.82(2)	1.109(9)
2e	0.266(2)	0.067	2.67(2)	1.051(8)
2f[a]	0.094(1)	0.239	2.60(2)	1.280(2)
$\sum$[b]	1.008	0.992		

[a] Two atomic positions. [b] The sum of the occupancies in the rows 2a–2f.

the final sums of all the refined occupancies approximately lead to the occupational probabilities of 0.5 : 0.5. Table 7 gives an overview over the refined occupational parameters and bond valence sums for the Pr^{3+} and Na^+ cations.

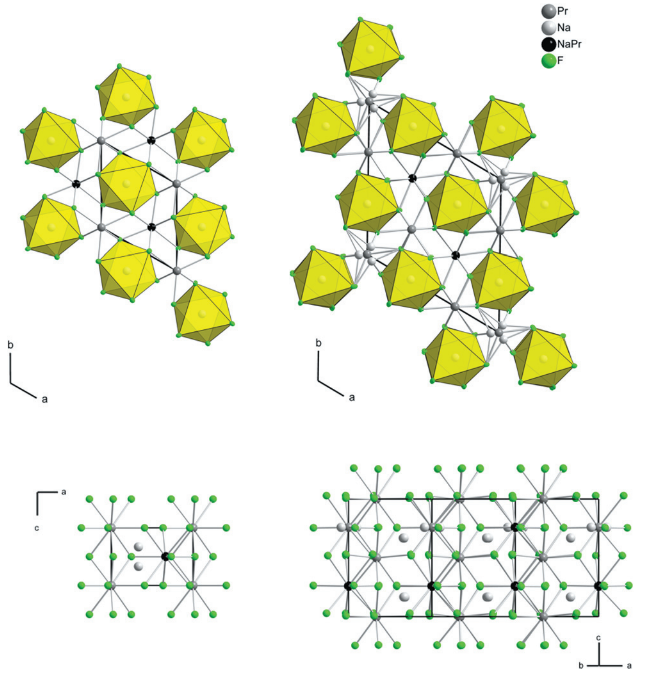

Fig. 1 Partial view of the average (left) and the superstructure (right) of $NaPrF_4$ at ambient pressure. The cation–oxygen distances smaller than 2.6 Å are shown. (Top) The view along the c axis. The NaF_6 octahedra are indicated in yellow. (Bottom) The view along the [010] and [$\bar{1}\bar{2}$0] directions, respectively. The NaF_6 octahedra are omitted for sake of clarity.

(4) In the β average structure, the Wyckoff position WP2h is only half occupied by Na^+. The Na^+ atomic positions are arranged in layers perpendicular to c at height $z \sim 0.17$ and 0.67. Taking into account the relevant group–subgroup relationship, this position splits into four symmetrically independent positions in the superstructure with space group symmetry $P3$. In the superstructure only two of them are fully occupied, the remaining two positions are completely empty, *i.e.*, an ordered distribution of Na atoms and vacancies exists. In other words, a layer of fully occupied Na^+ positions and a layer of vacancies alternate perpendicular to the c direction.

(5) For the atomic positions which correspond to the F1 and F2 positions in the average structure, deviations from the ideal positions are relatively small (0.121 Å for F1 and 0.201 Å for F2), yet significant.

Mean interatomic distances between the cations and oxygen atoms in the superstructure show small deviations from the ones in the average $P\bar{6}$ structure. For the cationic positions which are fully occupied by Pr, the mean Pr–F distances are 2.443(8) Å (Pr1a) and 2.411(8) Å (Pr1b) in the superstructure as compared to 2.426(4) Å in the average structure. For the cationic positions which are exclusively occupied by Na, a larger change is observed. While the mean distance in the average structure is 2.379(6) Å, the mean distance in the superstructure is significantly shorter −2.34(1) Å for Na1b. The average Na–F distance for Na1a remains essentially the same at−2.37(1) Å.

The mean distance between the oxygen atoms and the Na and Pr cations at the mixed sites (Pr2/Na2) is 2.490 (3) Å in the average structure, where the overall occupation is given by 50% of Pr and 50% of Na. As mentioned above, a part of the corresponding positions incorporate preferentially Pr, while others incorporate preferentially Na in the superstructure. As can be seen from Fig. 2, this is reflected in the mean distances in the superstructure as the mean (Pr2,Na2)–F distances correlate with the Pr^{3+} content (in %) at the cationic sites. For comparison, the values of the Pr1–F and Na1–F distances for the sites with 100%

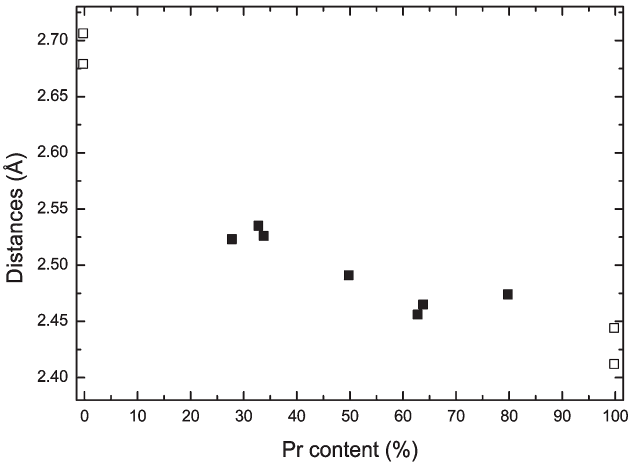

Fig. 2 Mean Pr–F distances in the $Pr2F_9$ polyhedra of the superstructure $NaPrF_4$ as a function of the Pr^{3+} content at ambient pressure. For comparison, the Pr1–F and Na1–F distances in the $Pr1F_9$ and $Na1F_{6+3}$ polyhedra, respectively, are also indicated (open symbols).

and 0% of Pr^{3+}, respectively, are also shown.¶ As can be seen, the mean distances clearly decrease with increasing Pr^{3+} content.

The superstructure of $NaPrF_4$ at ambient pressure has a higher degree of order than the average β structures. Our observations on the cation ordering within the superstructure can be compared with the modeling of diffuse scattering.[2] As pointed out by Aebischer *et al.*, the diffuse scattering at $l(2n + 1)/2$ is very sharp along c^* and can be explained by a real structure with translational order of Na^+ and Ln^{3+} at the position [WP1*f*] (2/3,1/3,1/2) in the average structure, meaning that the two cations alternate in the direction of *c*. The ordered columns are disordered in the (*a*,*b*) plane. The intensity distribution in the (a^*,b^*) plane can be modeled assuming a negative correlation between neighboring columns, *i.e.*, a column with Ln^{3+} at a given value of *z* will be preferably surrounded by columns with Na^+ at the same *z* value. Within our superstructure, six symmetrically independent cationic positions correspond to this *z* position. For all of the corresponding columns, a partial ordering in the direction of *c* can be observed. For four of these positions (2a–2d at $x = \pm1/3$, $y = \pm1/3$), the cationic position at $z \sim 0.25$ is preferentially occupied by Na^+ (approximately 66% of Na^+ and 33% of Pr^{3+}), while the situation is reversed for the position at $z \sim 0.75$. However, for the remaining 2 positions at $x \sim 0$ and $y \sim 0$, a higher degree of order is observed and the position at $z \sim 0.25$ is occupied by 80% of Pr^{3+}, the position at $z \sim 0.75$ is populated by about 72% of Na^+. In the latter position, Na^+ is slightly shifted from its ideal position on the 3-fold axis. The negative correlation between neighboring columns as described in ref. 2 is thus fully visible in the superstructure of $NaPrF_4$.

It was further pointed out in ref. 2 that, for a satisfactory modeling of the diffuse scattering, the F1 atoms have to be slightly shifted towards the trivalent rare earth cations in these columns. This is in good agreement with our refined superstructure of $NaPrF_4$ as the mean (Na,Pr)–F distances show a strong correlation with the respective occupation probabilities (Fig. 2). It should be noted in this context that the F2 atoms are also shifted towards the trivalent cations. This is reflected in the shorter cation–F2 distances when the sites are preferentially occupied by Pr^{3+} (Table 6)

The ordering of Na1 – the position [WP2*h*] (1/3,2/3,*z*) in the average structure and the position (2/3,2/3,*z*) in the superstructure (Fig. 1) – was, however, not considered in ref. 2 at all. In fact, the possibility of a partial or complete ordering of Na1 is not taken into account in the discussion of the diffuse scattering by Aebischer *et al.*, although it plays an essential part in the formation of the superstructure.

High-pressure data

Fig. 3 shows the pressure dependence of normalized lattice parameters and unit-cell volumes for β-$NaGdF_4$ and the superstructure $NaPrF_4$ from the single-crystal data and for β-$NaNdF_4$ from the powder data. All three materials are stable in the pressure range investigated here. Each of them is more compressible along the *a* axis. Their *P*–*V* compression data could be fitted with the second-order Birch–Murnaghan equations of state ($K' = 4.0$). The obtained zero-pressure bulk moduli and unit-cell volumes at ambient pressure are $B_0 = 72.4(3)$ GPa and $V_0 = 114.07(2)$ Å^3, $B_0 = 75.4(8)$ GPa and $V_0 = 732.5(3)$ Å^3, and $B_0 = 77.8(6)$ GPa and $V_0 = 120.03(5)$ Å^3, respectively. The differences in the bulk moduli are due to differences in the axial compressibilities in the *c* direction. Overall, these materials are more compressible than β-$NaYF_4$ for which $B_0 = 87$ GPa.[9]

It is remarkable that the hexagonal metrics of the β-$NaLnF_4$ compounds at ambient conditions can be converted into a pseudocubic one using *e.g.* the relationship $a_{\text{cubic}} = 1/3a_{\text{hex}} - 1/3b_{\text{hex}} + 2/3c_{\text{hex}}$, $b_{\text{cubic}} = 1/3a_{\text{hex}} + 2/3b_{\text{hex}} + 2/3c_{\text{hex}}$, $c_{\text{cubic}} = -2/3a_{\text{hex}} - 1/3b_{\text{hex}} + 2/3c_{\text{hex}}$. In particular, the deviations from the cubic metrics are minimal for the average structure of $NaPrF_4$: $a_{\text{cubic}} = 4.333$ Å and $\alpha = 90.05°$, $\beta = 89.96°$, $\gamma = 89.96°$. At 0.71 GPa,

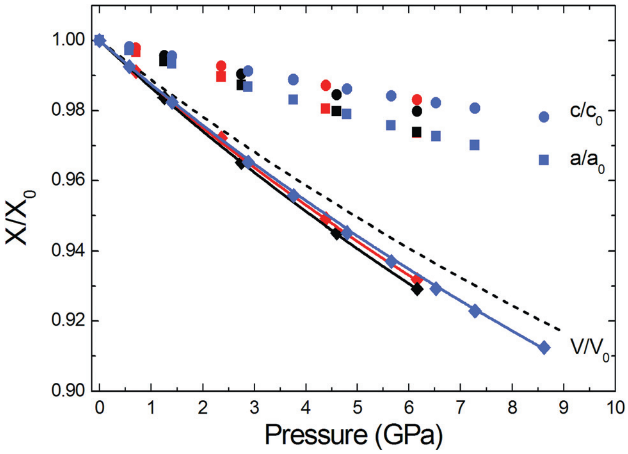

Fig. 3 Pressure dependence of normalized lattice parameters and unit-cell volumes in β-$NaNdF_4$ (blue symbols), β-$NaGdF_4$ (black symbols), and the superstructure $NaPrF_4$ (red symbols). The solid lines represent their Birch–Murnaghan equations of state. The dashed line stands for the Birch–Murnaghan equation of state of β-$NaYF_4$.[18]

¶The Na1–F distances discussed here include not only the six nearest fluorine neighbors of Na but also the next three fluorine atoms at considerably larger distances.

the metrics is even exactly cubic: $a_{\text{cubic}} = 4.321$ Å and $\alpha = \beta = \gamma = 90.00°$. Only at higher pressures is a significant deviation observed: $a_{\text{cubic}} = 4.233$ Å and $\alpha = \beta = \gamma = 89.68°$ at 6.16 GPa. For $NaGdF_4$, the metrics, which shows a significant deviation from the cubic one at ambient pressure ($a_{\text{cubic}} = 4.237$ Å, $\alpha = 89.08°$, $\beta = 90.92°$, $\gamma = 89.08°$), evolves in such a way that the deviations from the cubic metrics get smaller at higher pressures: $a_{\text{cubic}} = 4.134$ Å, $\alpha = 90.69°$, $\beta = 89.31°$, and $\gamma = 89.31°$ at 6.16 GPa.

All the high-pressure single-crystal data (Tables 8–13) were refined assuming the model of the average β structure – the Na^+ and the rare earth ions were treated anisotropically while the

Table 8 Experimental details for β-$NaGdF_4$ with the average structure at various pressures – space group $P\bar{6}$, $Z = 1$

Pressure (GPa)	1.25	2.75	4.60	6.16
Crystal data				
a (Å)	6.004(2)	5.963(2)	5.918(2)	5.882(4)
c (Å)	3.594(3)	3.575(2)	3.554(4)	3.537(6)
V (Å^3)	112.2(1)	110.09(8)	107.8(1)	106.0(2)
ρ(g cm^{-3})	5.69	5.80	5.92	6.02
λ (Å)	0.4000	0.4000	0.4000	0.4000
μ(mm^{-1})	4.810	4.902	5.007	5.093
G_{iso}	0.10(4)	0.13(4)	0.10(3)	0.11(3)
Data collection				
No. measured refl.	2052	1899	3693	2686
No. observed refl.[a]	402	427	446	409
$h_{\min}, h_{\max}$	−9,8	−10,10	−10,11	−8,8
$k_{\min}, k_{\max}$	−9,9	−8,10	−8,9	−9,9
$l_{\min}, l_{\max}$	−6,6	−6,6	−6,6	−6,6
$R(\text{int})_{\text{obs/all}}$[b]	9.08/9.09	8.77/8.78	7.92/7.92	8.06/8.06
Refinement				
$R_{\text{obs/all}}$	6.00/9.87	6.14/7.25	5.03/5.11	5.33/5.51
$wR_{\text{obs/all}}$	8.29/9.67	8.45/8.67	7.42/7.43	7.65/7.67
$\text{GoF}_{\text{obs/all}}$	6.68/6.05	5.90/5.94	5.68/5.74	5.72/5.81
No. parameters	15	15	15	15

[a] The criterion for observed reflections is $|F_{\text{obs}}| > 3\sigma$. [b] All agreement factors are given in %; weighting scheme $1/[\sigma^2(F_{\text{obs}})+(0.01F_{\text{obs}})^2]$.

Table 9 Atomic coordinates and isotropic displacement parameters in β-$NaGdF_4$ with the average structure at ambient pressure (0.0001 GPa), 1.25, 2.75, 4.60, and 6.16 GPa – space group $P\bar{6}$, $Z = 1$

Pressure (GPa)	Atom	x	y	z	Occ.	U_{iso}
0.0001	Gd1	0	0	0	1	0.0100(1)
1.25	Gd1	0	0	0	1	0.0118(3)
2.75	Gd1	0	0	0	1	0.0117(3)
4.60	Gd1	0	0	0	1	0.0111(2)
6.16	Gd1	0	0	0	1	0.0121(3)
0.0001	Na1	1/3	2/3	0.581(3)	0.5	0.020(2)
1.25	Na1	1/3	2/3	0.595(6)	0.5	0.012(3)
2.75	Na1	1/3	2/3	0.579(5)	0.5	0.016(3)
4.60	Na1	1/3	2/3	0.579(4)	0.5	0.014(2)
6.16	Na1	1/3	2/3	0.581(5)	0.5	0.020(3)
0.0001	Na2/Gd2	2/3	1/3	1/2	0.5/0.5	0.0047(1)
1.25	Na2/Gd2	2/3	1/3	1/2	0.5/0.5	0.0050(4)
2.75	Na2/Gd2	2/3	1/3	1/2	0.5/0.5	0.0037(4)
4.60	Na2/Gd2	2/3	1/3	1/2	0.5/0.5	0.0040(3)
6.16	Na2/Gd2	2/3	1/3	1/2	0.5/0.5	0.0030(3)
0.0001	F1	0.6304(6)	0.0406(7)	0	1	0.028(1)
1.25	F1	0.648(4)	0.069(4)	0	1	0.025(3)
2.75	F1	0.647(4)	0.061(3)	0	1	0.026(3)
4.60	F1	0.633(4)	0.051(4)	0	1	0.030(3)
6.16	F1	0.636(6)	0.056(5)	0	1	0.042(4)
0.0001	F2	0.7308(4)	0.7536(4)	1/2	1	0.0152(6)
1.25	F2	0.718(3)	0.747(2)	1/2	1	0.017(2)
2.75	F2	0.720(2)	0.751(2)	1/2	1	0.012(2)
4.60	F2	0.726(2)	0.748(2)	1/2	1	0.012(1)
6.16	F2	0.726(2)	0.751(1)	1/2	1	0.007(1)

Table 10 Selected distances (Å) in β-$NaGdF_4$ with the average structure at ambient pressure (0.0001 GPa), 1.25, 2.75, 4.60, and 6.16 GPa – space group $P\bar{6}$, $Z = 1$

Pressure (GPa)					
0.0001	Gd1	–F1	(3×)	2.340(9)
	1.25	Gd1	–F1	(3×)	2.35(3)
	2.75	Gd1	–F1	(3×)	2.31(3)
	4.60	Gd1	–F1	(3×)	2.34(2)
	6.16	Gd1	–F1	(3×)	2.32(4)
	0.0001	Gd1	–F2	(6×)	2.381(4)
	1.25	Gd1	–F2	(6×)	2.42(1)
	2.75	Gd1	–F2	(6×)	2.39(1)
	4.60	Gd1	–F2	(6×)	2.36(1)
	6.16	Gd1	–F2	(6×)	2.35(1)
	0.0001	Na1	–F1	(3×)	2.601(9)
	1.25	Na1	–F1	(3×)	2.64(2)
	2.75	Na1	–F1	(3×)	2.63(2)
	4.60	Na1	–F1	(3×)	2.55(2)
	6.16	Na1	–F1	(3×)	2.56(3)
	0.0001	Na1	–F2	(3×)	2.220(5)
	1.25	Na1	–F2	(3×)	2.14(2)
	2.75	Na1	–F2	(3×)	2.12(1)
	4.60	Na1	–F2	(3×)	2.14(1)
	6.16	Na1	–F2	(3×)	2.12(2)
	0.0001	(Na2,Gd2)	–F1	(6×)	2.440(6)
	1.25	(Na2,Gd2)	–F1	(6×)	2.36(2)
	2.75	(Na2,Gd2)	–F1	(6×)	2.38(2)
	4.60	(Na2,Gd2)	–F1	(6×)	2.38(2)
	6.16	(Na2,Gd2)	–F1	(6×)	2.35(2)
	0.0001	(Na2,Gd2)	–F2	(3×)	2.363(5)
	1.25	(Na2,Gd2)	–F2	(3×)	2.35(2)
	2.75	(Na2,Gd2)	–F2	(3×)	2.35(1)
	4.60	(Na2,Gd2)	–F2	(3×)	2.30(1)
	6.16	(Na2,Gd2)	–F2	(3×)	2.30(1)

Table 11 Experimental details for β-$NaPrF_4$ with the average structure at various pressures – space group $P\bar{6}$, $Z = 1$

Pressure (GPa)	0.71	2.23	4.39	6.16
Crystal data				
a (Å)	6.110(2)	6.067(2)	6.011(2)	5.969(4)
c (Å)	3.742(3)	3.722(2)	3.702(4)	3.686(6)
V (Å^3)	121.0	118.6	115.8	113.7
ρ(g cm^{-3})	4.94	5.03	5.16	5.25
λ (Å)	0.4000	0.4000	0.4000	0.4000
μ(mm^{-1})	3.186	3.261	3.34	3.401
G_{iso}	0.13(3)	0.15(2)	0.16(2)	0.17(2)
Data collection				
No. measured refl.	2172	2175	1977	2451
No. observed refl.[a]	431	478	488	470
$h_{\min}, h_{\max}$	−11,9	−11,11	−11,11	−11,11
$k_{\min}, k_{\max}$	−10,11	−11,11	−11,11	−11,11
$l_{\min}, l_{\max}$	−5,3	−5,5	−5,5	−5,5
$R(\text{int})_{\text{obs/all}}$[b]	10.30/10.33	10.01/10.05	10.01/10.04	10.06/10.08
Refinement				
$R_{\text{obs/all}}$	5.91/6.09	5.47/5.83	5.39/5.66	4.92/5.19
$wR_{\text{obs/all}}$	6.14/6.16	5.50/5.52	5.75/5.78	5.31/5.36
$\text{GoF}_{\text{obs/all}}$	3.63/3.66	3.06/3.11	3.22/3.25	3.10/3.11
No. parameters	15	15	15	15

[a] The criterion for observed reflections is $|F_{\text{obs}}| > 3\sigma$. [b] All agreement factors are given in %; weighting scheme $1/[\sigma^2(F_{\text{obs}})+(0.01F_{\text{obs}})^2]$.

Table 12 Atomic coordinates and isotropic displacement parameters in β-$NaPrF_4$ with the average structure at ambient pressure (0.0001 GPa), 0.71, 2.36, 4.39, and 6.16 GPa – space group $P\bar{6}$, $Z = 1$

Pressure (GPa)	Atom	x	y	z	Occ.	U_{iso}
0.0001	Pr1	0	0	0	1	0.00787(4)
0.71	Pr1	0	0	0	1	0.0088(3)
2.36	Pr1	0	0	0	1	0.0080(2)
4.39	Pr1	0	0	0	1	0.0080(2)
6.16	Pr1	0	0	0	1	0.0082(2)
0.0001	Na1	1/3	2/3	0.670(3)	0.5	0.032(2)
0.71	Na1	1/3	2/3	0.693(9)	0.5	0.030(7)
2.36	Na1	1/3	2/3	0.705(11)	0.5	0.050(9)
4.39	Na1	1/3	2/3	0.738(13)	0.5	0.059(9)
6.16	Na1	1/3	2/3	0.720(12)	0.5	0.07(1)
0.0001	Na2/Pr2	2/3	1/3	1/2	0.5/0.5	0.01060(9)
0.71	Na2/Pr2	2/3	1/3	1/2	0.5/0.5	0.0117(7)
2.26	Na2/Pr2	2/3	1/3	1/2	0.5/0.5	0.0120(6)
4.39	Na2/Pr2	2/3	1/3	1/2	0.5/0.5	0.0132(6)
6.16	Na2/Pr2	2/3	1/3	1/2	0.5/0.5	0.0132(6)
0.0001	F1	0.6334(6)	0.0409(7)	0	1	0.024(1)
0.71	F1	0.628(2)	0.038(2)	0	1	0.021(2)
2.26	F1	0.627(2)	0.040(2)	0	1	0.018(2)
4.39	F1	0.628(2)	0.04582)	0	1	0.022(2)
6.16	F1	0.626(2)	0.045(2)	0	1	0.020(2)
0.0001	F2	0.7328(5)	0.7552(4)	1/2	1	0.0138(6)
0.71	F2	0.732(2)	0.753(1)	1/2	1	0.014(1)
2.26	F2	0.729(2)	0.750(1)	1/2	1	0.018(2)
4.39	F2	0.721(2)	0.747(1)	1/2	1	0.020(2)
6.16	F2	0.719(2)	0.749(1)	1/2	1	0.020(2)

Table 13 Selected distances (Å) in β-$NaPrF_4$ with the average structure at ambient pressure (0.0001 GPa), 0.71, 2.36, 4.39, and 6.16 GPa – space group $P\bar{6}$, $Z = 1$

Pressure (GPa)				
0.0001	Pr1	–F1	(3×)	2.383(5)
0.71	Pr1	–F1	(3×)	2.40(1)
2.36	Pr1	–F1	(3×)	2.40(1)
4.39	Pr1	–F1	(3×)	2.38(2)
6.16	Pr1	–F1	(3×)	2.38(2)
0.0001	Pr1	–F2	(6×)	2.448(2)
0.71	Pr1	–F2	(6×)	2.447(8)
2.36	Pr1	–F2	(6×)	2.443(7)
4.39	Pr1	–F2	(6×)	2.449(8)
6.16	Pr1	–F2	(6×)	2.438(8)
0.0001	Na1	–F1	(3×)	2.440(7)
0.71	Na1	–F1	(3×)	2.37(2)
2.36	Na1	–F1	(3×)	2.34(2)
4.39	Na1	–F1	(3×)	2.29(2)
6.16	Na1	–F1	(3×)	2.30(2)
0.0001	Na1	–F2	(3×)	2.317(4)
0.71	Na1	–F2	(3×)	2.33(2)
2.36	Na1	–F2	(3×)	2.32(2)
4.39	Na1	–F2	(3×)	2.31(2)
6.16	Na1	–F2	(3×)	2.25(2)
0.0001	(Na2,Pr2)	–F1	(6×)	2.531(3)
0.71	(Na2,Pr2)	–F1	(6×)	2.52(1)
2.36	(Na2,Pr2)	–F1	(6×)	2.50(1)
4.39	(Na2,Pr2)	–F1	(6×)	2.446(9)
6.16	(Na2,Pr2)	–F1	(6×)	2.50(1)
0.0001	(Na2,Pr2)	–F2	(3×)	2.409(3)
0.71	(Na2,Pr2)	–F2	(3×)	2.39(1)
2.36	(Na2,Pr2)	–F2	(3×)	2.36(1)
4.39	(Na2,Pr2)	–F2	(3×)	2.34(1)
6.16	(Na2,Pr2)	–F2	(3×)	2.34(1)

fluorine ions were treated isotropically. As can be seen from Tables 9 and 12, changes in the atomic coordinates as a function of pressure are very small and hardly significant. An inspection of Tables 10 and 13 reveals that the bulk compressibility of the average structure predominantly results from the contraction of the distorted octahedra around the Na1 atoms.

Trials to refine the superstructure $NaPrF_4$ on compression were unsuccessful as the adjustment of the weak superstructure reflections failed. We ascribe this to the fact that at high pressures the enhanced background due to the components of the diamond anvil cell falsifies the intensities of the weak reflections in this material so strongly that their measured values are not reliable. However, we did not observe that the visible superstructure reflections vanish or decrease in intensity, nor did we see any new reflections appear when pressure is increased. Hence, we did not find any indication that the superstructure is unstable with respect to pressure-induced ordering of the cations in the conditions studied here. Such a behavior is similar to that of β-$NaYF_4$, which is stable to about 20 GPa.[9]

Conclusions

We studied the $NaLnF_4$ materials (Ln = La, Ce, Pr, Nd, Sm and Gd) using synchrotron single-crystal diffraction. The compounds with Ln = La, Ce, Nd, Sm, and Gd crystallize in the β structure previously reported.[2,9,14] A new type of superstructure due to partial ordering of the Na^+ and Pr^{3+} cations as well as of vacancies is observed in $NaPrF_4$. The structural model could be derived on the basis of group–subgroup relationships $P\bar{6} \leftrightarrow P3$. The high-pressure studies using synchrotron powder and single-crystal diffraction in diamond anvil cells at room temperature demonstrate that β-$NaNdF_4$ and β-$NaGdF_4$ as well as the superstructure $NaPrF_4$ are stable on compression to at least 8 GPa.

Several of the crystals studied here (Ln = La, Ce, Pr, Sm, and Gd) came from exactly the same synthesis batches that were previously investigated with vibrational spectroscopy by Lage *et al.* in the year 2005,[14] who did not detect any spectral features that contradict the model of the average β structure. This observation might thus imply that the average β structure is in fact unstable and that the ordering of the cations and vacancies is a slow process at atmospheric pressure. If so, order–disorder transformations would have a profound influence over the luminescent properties of these materials when doped. One might speculate that further disorder–order transformations of the superstructure $NaPrF_4$ presented here might follow the group–subgroup relations. Therefore, the whole issue of ordering of the cations and vacancies in the $NaXF_4$ materials requires further investigations.

Acknowledgements

Crystals for this work were kindly provided by Jean-Yves Gesland (Le Mans, France). We thank M. Tolkiehn for his technical assistance at DESY. Portions of this research were carried out at the light source DORIS III at DESY which is a member of the Helmholtz Association (HGF). The research leading to these results has received funding from the European Community's Seventh Framework Programme (FP7/2007–2013) under grant agreement no. 226716.

References

1 M. Haase and H. Schäfer, *Angew. Chem., Int. Ed.*, 2011, **50**, 5808.
2 A. Aebischer, M. Hostettler, J. Hauser, K. Krämer, T. Weber, H. U. Göbel and H. B. Bürgi, *Angew. Chem., Int. Ed.*, 2006, **45**, 2802.
3 C. Renero-Lecuna, R. Martin-Rodriguez, R. Valiente, J. González, F. Rodriguez, K. W. Krämer and H. U. Güdel, *Chem. Mater.*, 2011, **23**, 3442.
4 J. H. Burns, *Inorg. Chem.*, 1965, **4**, 881.
5 R. E. Thoma, H. Insley and G. M. Herbert, *Inorg. Chem.*, 1966, **5**, 1222.
6 A. Grzechnik, K. Syassen, I. Loa, M. Hanfland and J.-Y. Gesland, *Phys. Rev. B: Condens. Matter*, 2002, **65**, 104102.
7 A. Grzechnik, W. A. Crichton, P. Bouvier, V. Dmitriev, H.-P. Weber and J.-Y. Gesland, *J. Phys.: Condens. Matter*, 2004, **16**, 7779.
8 A. Grzechnik, K. Friese, V. Dmitriev, H.-P. Weber, J.-Y. Gesland and W. A. Crichton, *J. Phys.: Condens. Matter*, 2005, **17**, 763.
9 A. Grzechnik, P. Bouvier, M. Mezouar, M. D. Mathews, A. K. Tyagi and J. Köhler, *J. Solid State Chem.*, 2002, **165**, 159.
10 A. Grzechnik, P. Bouvier, W. A. Crichton, L. Farina and J. Köhler, *Solid State Sci.*, 2002, **4**, 895.
11 O. V. Frank-Kamenetskaya, V. S. Fundamenskii, A. K. Tsytsenko and V. A. Frank-Kamenetskii, *Crystallogr. Rep.*, 1994, **39**, 923.
12 A. Grzechnik, M. Fechtelkord, W. Morgenroth, J. M. Posse and K. Friese, *J. Phys.: Condens. Matter*, 2007, **19**, 266219.
13 W. H. Zachariasen, *Acta Crystallogr.*, 1948, **1**, 265.
14 M. M. Lage, R. L. Moreira, F. M. Matinaga and J.-Y. Gesland, *Chem. Mater.*, 2005, **17**, 4523.
15 H. Ahsbahs, *Z. Kristallogr.*, 2004, **219**, 305.
16 R. Boehler, *Rev. Sci. Instrum.*, 2006, **77**, 115103.
17 W. Kabsch, *Acta Crystallogr., Sect. D: Biol. Crystallogr.*, 2010, **66**, 125.
18 K. Friese, Y. Kanke and A. Grzechnik, *Acta Crystallogr., Sect. B: Struct. Sci.*, 2009, **65**, 326.
19 J. M. Posse, K. Friese and A. Grzechnik, *J. Phys.: Condens. Matter*, 2011, **23**, 215401.
20 V. Petricek, M. Dusek and L. Palatinus, *JANA2006 – Crystallographic Computing System*, Institute of Physics, Academy of Sciences of the Czech Republic, Praha, 2006.
21 A. P. Hammersley, S. O. Svensson, M. Hanfland, A. N. Fitch and D. Hausermann, *High Pressure Res.*, 1996, **14**, 235.
22 R. J. Angel, *J. Phys.: Condens. Matter*, 1993, **5**, L141.
23 H. K. Mao, J. Xu and P. M. Bell, *J. Geophys. Res.*, 1986, **91**, 4673.
24 W. C. Hamilton, *Statistics in Physical Science*, Ronald Press Company, New York, 1964.
25 W. C. Hamilton, *Acta Crystallogr.*, 1965, **18**, 823.
26 A. Grzechnik, W. Morgenroth and K. Friese, *J. Solid State Chem.*, 2009, **182**, 1792.
27 K. Friese, W. Morgenroth, J. M. Posse and A. Grzechnik, *Dalton Trans.*, 2011, **40**, 1902.
28 B. J. Campbell, H. T. Stokes, D. E. Tanner and D. M. Hatch, *J. Appl. Crystallogr.*, 2006, **39**, 607.